SCIREA Journal of Materials
http://www.scirea.org/journal/Materials
November 30, 2021
Volume 6, Issue 4, August 2021
https://doi.org/10.54647/materials43154

Study on effect of Cu integration and Oxygen vacancy/defect creation in electronic properties of TiO_2 photocatalyst using first principles calculations

R. Gandhimathi[1], R. Vidhya[2,] *, R. Karthikeyan[3]

[1] Nanophotonics Research Laboratory, Department of Physics, AMET University, Chennai, India (https://orcid.org/0000-0003-0013-962X)

[2] Department of Physics, V.V.Vanniaperumal College for Women, Virudhunagar, India.

[3] Department of Physics, Anna University Regional Campus, Tirunelveli, India

* Corresponding author: E-mail: crystgandhi@gmail.com

Abstract

In this investigation, it was proposed to analyze the optimized geometry, density of states (DOS) and electronic band structures of copper (4.16%, 4.16%+oxygen vacancy & 8.33%) doped Titanium Dioxide (Cu-TiO_2) photocatalysts using density functional theory corrected for on-site Coulombic interactions (DFT+U). The photocatalytic reactivity of pristine TiO_2 material is limited because of its wider bandgap and faster excitons recombination. Nevertheless, the transition metal ions doping like Cu ions reduce the energy requirement for electronic transition and thereby a maintain higher redox potential which might enhance the catalytic efficiency. DFT+U calculations revealed that inserting Cu atom modifies the band gap distribution and forms new unoccupied energy levels in the band gap near the top of valence band due to hybridization of Cu 3d states with Ti 3d states. The first principles calculations showed that the charge compensating oxygen vacancies form adjacent to the

conduction band. Also, the oxygen vacancy creation brings modification in coordination geometry and makes the possibility of tuning the optical and catalytical properties of Cu doped TiO_{2-x} material intensely.

Keywords: DFT, Cu-TiO_2, Hubbard U correction, Oxygen vacancy

1. Introduction

The transition metal oxide semiconductor TiO_2 is an essential and a widely used material in most of the industrial products like sunscreen, paints, coatings, and self-cleaning glasses because of its high photoactive ability [1,2]. Besides, more research works are going on TiO_2 materials because of its abundant, non-toxic, economically cheap, and thermally and chemically stable in nature. Catalytic oxidation and reduction processes are one of the possible remediations to solve the environmental pollution issues. TiO_2 semiconductor photocatalyst is a well-known commercially available catalyst material. Still, the wider band gap (3.2eV), high energy requirement for exciton generation & faster rate of recombination of excitons of TiO_2 photocatalyst hold back its extended benefits in the fields of photocatalytic and photovoltaic applications [3]. Lots of research articles have been published on improving its quantum efficiency (conversion of absorbed photon to electron generation) and increasing lifetime of photogenerated excitons by metal and non-metal impurity ions doping. In such a context, transition metal ions doping into the TiO_2 matrix influences the photon absorption ability and modifies the band gap of pristine TiO_2 significantly [4,5]. Cu dopant at the anatase TiO_2 surface exhibits enhanced photocatalytic activity under sunlight or visible light irradiation [6]. It displays excellent electron-hole separation with photo excitation as well it preserves the association of adsorbed water to hydroxyls better than other transition metals [7-9]. Another way to improve the catalytic efficiency of TiO_2 material is the creation of point defects or lattice defects in the TiO_2 system which can modulate the light photon absorption ability and photo catalytic reaction of TiO_2 in a remarkable way. Oxygen vacancy defects are obvious in TiO_2 matrix during synthesis and materials preparation. However, these defects serve as adsorption sites for pollutant reactants and enhance the rate of photocatalytic reaction.

To refine the electronic properties of TiO_2 photocatalyst, an optimization of the band structure is mandatory. Therefore, we focus on streamlining the process of narrowing the bandgap, Eg (improves visible light absorption), that is proper positioning of the valence band and the

conduction band into the system [10]. The theoretical simulation on TiO_2 and metal doped TiO_2 semiconductor is obligatory for eventual understanding and designing materials for advanced technology since the results from the first-principles calculations would be more supportive to give greater understanding about the electronic band structure of TiO_2 material.

In this work, the impacts of transition metal ions incorporation and lattice defects or oxygen vacancies creation into TiO_2 matrix were investigated via the first principles calculations based on the density functional theory (DFT) study. DFT is a computational quantum mechanical modelling that describes the quantum behavior of atoms and molecules employing functionals of spatially dependent electron density [11-13]. The main advantage of this method is that it reduces the quantum mechanical ground state many-electron problem to self-consistent one-electron form, through the Kohn-Sham equations [14]. Moreover, DFT is an ideal method for the calculation of the electronic band structure, optical properties, and potential energy surface of the smallest chemical systems [15] in consideration with their structural and cohesive properties. However, it shows few discrepancies in the prediction of electronic bandgap values. One of the corrective approaches employed to dissolve the DFT electronic bandgap problem is the GGA+U correction method. The U correction leads to the strong on-site Coulomb interaction of localized electrons with an additional Hubbard-like term and describes the strongly correlated electronic states (d and f orbitals), while treating the rest of the valence electrons by the normal DFT approximations [16]. Here the mechanism of band gap narrowing, and the associated optical properties have been conferred. The main idea of this work is execution of the planewave ultra-soft pseudopotential method within the framework of density functional theory (DFT) to reveal the reactive mechanism and to optimize the doping concentration value which determines the performance of Cu doped TiO_2 photocatalyst under visible light irradiation.

1.1 Methodology

1.1.1 Density functional theory

First principles density functional theory (DFT) permits the calculation and prediction of material properties directly from quantum mechanical considerations. The single electron Schrodinger wave equation with the potential V(r) is given by

$$\hat{H}\psi_n(r) = \left[-\frac{\hbar^2}{2m}\nabla^2 + V(r) \right] \psi_n(r) = E_i \psi_n(r)$$

$\hat{H}$ -single electron Hamiltonian, E_i energy eigen values, and $\psi_n(r)$ -wave functions. It describes the quantum state of a set of particles in an isolated system, r-position vectors. By solving the Schrodinger wave equation, the ground-state energy, Eg, of the material (energy of most stable state of a system) can be calculated. The ground-state energy is a function of the electron density ρ (r) (which has lattice periodicity), external potentials V(r) and the ground-state expectation value of Hamiltonian (H_0) is F [ρ(r)].

$$E_g < \int drV(r)\rho(r) + F[\rho(r)]$$

The electron density that minimizes the energy of the overall functional is known as the true state electron density. According to Hohenberg Kohn, it is sufficient to know the electron density of a system to determine its total energy [17-23]. The Kohn–Sham equations related the electron density to wavefunctions of non-interacting electrons by

$$\rho(r) = \sum_{n=1}^{N} \psi_n^*(r)\psi_n(r)$$

and F [ρ(r)].is written as

$$F[\rho(r)] = E_k[\rho(r)] + E_H[\rho(r)] + E_{XC}[\rho(r)]$$

where E_k is the kinetic energy for the system of noninteracting electrons that produce ρ(r), E_H is the Hartree–Coulomb energy, and E_{xc} is the exchange–correlation energy and it is the measure of how much the movement of one electron is influenced by the presence of all other electrons. Also, it depends on electron density distribution completely. The KS potential is built from parts that are exactly known as the external potential, Hartree potential and exchange-correlation (EXC) potential. The effective potential in the Kohn–Sham methodology is then given by

$$V_{KS}(\rho(r)) = \frac{\delta}{\delta\rho(r)}(E_H[\rho(r)]) = V_H\rho(r) + \frac{\delta E_{XC}[\rho(r)]}{\delta\rho(r)}$$

Exchange correlation potential $V_{XC}(r) = \dfrac{\delta E_{XC}[\rho(r)]}{\delta\rho(r)}$

Self-consistency of Kohn-Sham states

$$\left(-\frac{\hbar^2}{2m}\nabla^2 + V(\vec{r}) + V_H(\vec{r}) + V_{XC}(\vec{r})\right)\psi_n(r) = E_i\psi_n(r)$$

To closely approximate a solution to the Kohn–Sham equations, the exchange–correlation energy, Exc, is introduced in the form described in the local-density approximation

(LDA):

$$E_{XC}^{LDA}[\rho(\vec{r})] = \int d\vec{r}\,\rho(\vec{r})E_{XC}[\rho(\vec{r})]$$

where E_{xc} is the exchange–correlation energy per electron

LDA assumes electron gas is homogeneous locally, so that exchange correlation energy depends only on the local electron density around each volume element dr in the system.

$$E_{XC}^{GGA}[\rho(\vec{r})] = E_{XC}^{LDA}[\rho(\vec{r})] + \Delta E_{XC}\left[\frac{\nabla\rho(r)}{\rho^{4/3}(r)}\right]$$

GGA includes gradient corrections to the electron density and does a better job for most things, especially less dense systems like molecules bonding to oxide surfaces ionic and covalent crystals etc. GGA reduce the LDA error in the atomization energy significantly [24-28]. Fundamentally, it is a cost-effective method for conducting the DFT calculations.

1.1.2 Fermi Energy

Fermi level governs the charge carrier population according to the integral over density of states times Fermi Dirac distribution.

$$N = \int_0^\infty g(E)f(E)dE$$

g(E)-density of states

The Fermi function f(E) gives the probability that an energy state is full.

$$f(E) = \frac{1}{1+e^{(E-E_f)}/K_BT}$$

K_B -Boltzmann constant -1.38×10^{-23} J/K

For the valence and conduction bands the Fermi function can be written as

$$f(E_V) = \frac{1}{1+e^{(E_V-E_f)}/K_BT},\quad f(E_C) = \frac{1}{1+e^{(E_C-E_f)}/K_BT}$$

The probability that the state is empty

$$1 - f(E_V) = \frac{1}{1 + e^{(E_f - E_V)} / K_B T}$$

2. Computational details

The total energy calculation and geometry optimizations has been performed by using a plane-wave basis set and ultrasoft pseudopotentials [29-31] as implemented in the Quantum-ESPRESSO package. The exchange–correlation (XC) functional used was ultra-soft pseudopotentials with Perdew–Burke–Ernzerhof (PBE) scheme [32,33]. Exchange and correlation energy is defined as the energy difference between the exact total energy of a system and the classical Hartree energy. The assigned gradient approximation for DFT method is Generalized gradient approximation (GGA)+U. The GGA approximations to Exchange and correlation energy make the functional depend on both the electron density and the gradient of the density since electron density can vary rapidly over a small region of space. Ultrasoft pseudopotential (USP) method defines the interaction between ions and electron and make faster calculations. Besides, it allows performing the calculations at lowest possible cutoff energy for the plane-wave basis set. We can attain much smoother (softer) pseudo-wavefunctions even with fewer plane-waves for calculations to obtain higher accuracy. In other words, a soft potential for valence electrons only (core electrons disappear from the calculation) having pseudo-wavefunctions containing no "orthonormality wiggles". In many systems, Norm Conserving Pseudopotentials allow accurate calculations with moderate-size (Ec ~ 10 − 20Ry) plane-wave basis sets. The GGA with Hubbard parameter (U) advance the extrapolation of ground state properties and electronic structure of the TiO_2 with respect to the conventional GGA. The GGA+*U* method also allows a correct prediction of phase stability at high pressure [34]. Here the model structures used are Pristine TiO_2 (SYS-1), 4.17% Cu+TiO_2 (SYS-2), 4.17% Cu+ Oxygen Vacancy +TiO_2 (SYS-3), and 8.33%Cu+TiO_2 (SYS-4). In all the four model structures, two-unit cells of anatase phase TiO_2 were put together along 'a' axis with the supercell dimension of $2 \times 1 \times 1$. The number of atoms present in all four structures are 24 atoms. The spheres in grey color represent Ti-atoms where red and green spheres represent O and Cu atoms respectively. To understand the influence of substitutional impurity in the anatase phase TiO_2, the Cu dopants of different concentration have been introduced into the Ti lattice sites to produce three different configurations such as SYS-2, SYS-3, and SYS-4. In SYS-2, one Ti atom has been replaced by a Cu atom i.e.,4.17 atomic%

of Cu dopant. In SYS-3 model, one Ti atom was replaced by a Cu atom along with one oxygen vacancy creation i.e.,4.17 atomic % of Cu plus V_o -Oxygen vacancy. As well, two Ti atoms are replaced by 2 Cu atoms in SYS-4structure i.e., 8.33 atomic % of Cu.

3. Results and Discussions

3.1 Geometry optimization

To determine the molecular structure or to find an atomic arrangement in the unit cell, the geometry optimization study need to be carried out. It can give the atomic arrangement which makes the molecule most stable. For geometry optimization, the total energy and its first derivatives with respect to ionic coordinates are to be minimized by the displacement of ionic positions. Geometry optimization calculations were performed on the pristine TiO_2 (SYS-1), as well the doped systems SYS-2, SYS-3, and SYS-4, for allowing all atoms to relax. The optimized structure of pristine and Cu doped TiO_2 are shown in Fig.1. All the structures were found as relaxed. It is noticed that the modelled structures show no variation in the lattice parameters. The standard DFT methods undervalue the band gap, whereas GGA+U, because of the contribution of exact exchange in the exchange functional provide values in closer agreement with experiments. The general gradient approximation (GGA) + U (Hubbard coefficient) method has been adopted to describe the exchange-correlation effects accurately. For oxide materials the suggested U value is ~7 eV for first principles calculations [35]. Hence an optimized Hubbard correction term U=7.5eV in the conventional GGA has been introduced to stabilize the phase of TiO_2 effectively. The convergence threshold set for ionic minimization/relaxation is 10^{-6} eV. The total force on the pure TiO_2 system was found as 0.001925Ry/Bohr. Cu dopant in Cu^{2+} valence might occupy as a substitutional impurity ion by replacing Ti^{4+} ion. The photo excited electron facilitates the reduction of Cu^{2+} into Cu^{+} thus extending the lifetime of positive charge carriers which is a perquisite for enhanced catalytic activity.

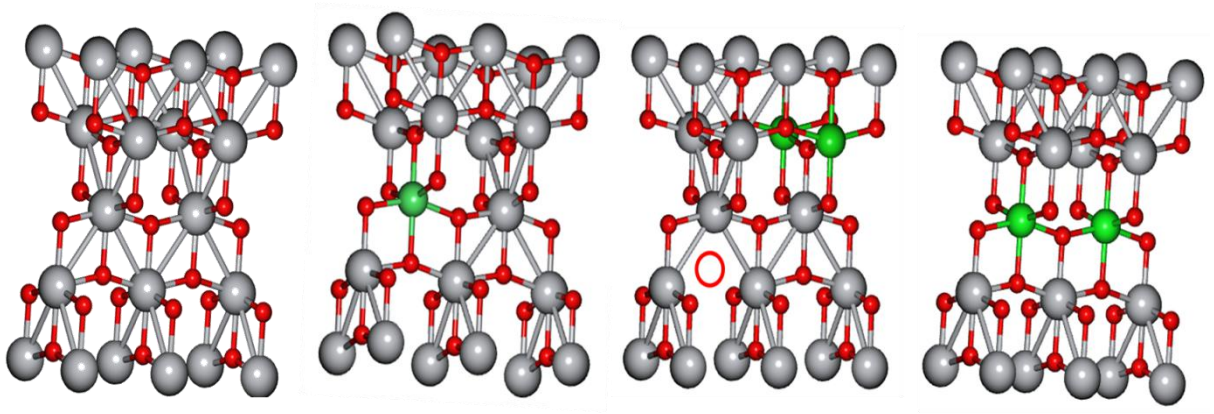

Fig.1 Geometry optimized structure of
a) Pristine TiO_2 (b) SYS-2 (c) SYS-3 (d) SYS-4

3.2 Density of states (DOS)

The density of states calculation offers geometric information on the state's availability at each energy level. A high value for the density of states signifies a high number of energetic states ready to be occupied. If there are no available states for occupation in an energetic level, the value for the density of states will be zero where the zero-point energy represents the Fermi level. In such a way in pristine TiO_2, it defines the occupation of titanium (Ti) and oxygen (O) atoms at each energy level. The schematic diagrams of band structure and p-d orbitals hybridization are shown in Fig.2a and 2b respectively.

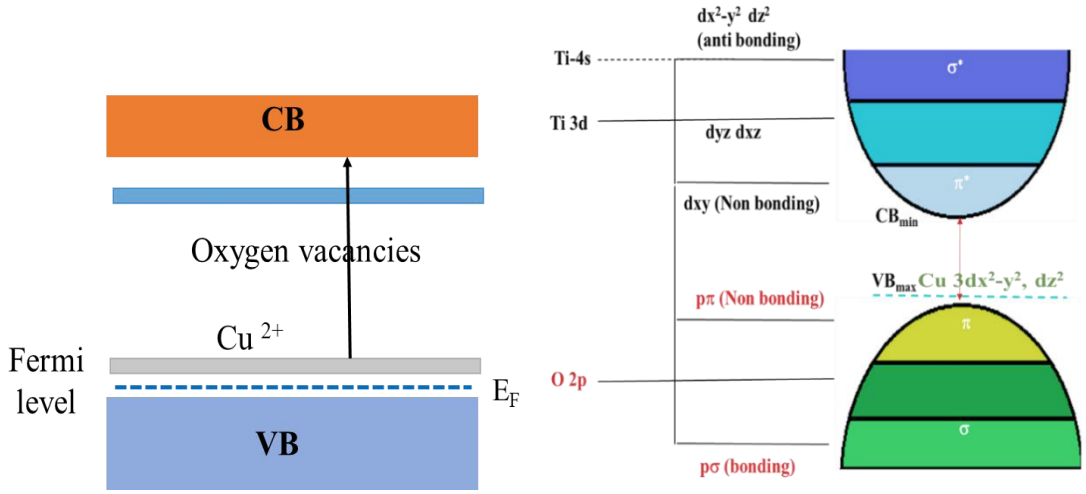

Fig.2a & 2b Schematic diagram p-d orbitals hybridization

The calculated DOS and Partial DOS of modelled pristine TiO_2 and Cu doped TiO_2 materials are shown in Fig.3a and 3b. The DOS showed that in pristine TiO_2 (SYS-1), Ti-($4s^2$ $3d^2$) and O-($2p^4$) valence electrons take part in p-d molecular orbital hybridization. Hence the valence band is dominated by O 2p orbitals (fully occupied) and the conduction band is dominated by

Ti 3d orbitals (unoccupied). Nevertheless, the integration of the Cu atom significantly alters the DOS, further inducing variations in both the valence band and conduction band characters with the increase of dopant concentration. The Cu substitutional impurity ions create empty levels (Cu, $3dx^2$-y^2, dz^2 states) near the top of valence band about ~0.5eV. The delocalized 3d states of Cu dopant contributes to the creation of impurity energy level by hybridizing with O 2p states or Ti 3d states which provide a trapping potential well for photo induced holes and delay the recombination of excitons in a substantial way [36]. It is also observed that the width of valence band is ~4.8eV in pure TiO_2. However, the doped samples demonstrate increase in the width of the valence band by ~1.3eV. The TDOS shape of Cu doped TiO_2 turn into broader than that of pure TiO_2 which lead to reduction of band gap of Cu doped TiO_2 materials. In all the doped samples, the reduction in the band gap is attributed to the grouping of Cu 3d and O 2p states above the valence band maximum [37]. Similarly, in SYS-3, the impact of oxygen vacancy creation, and 3d metal ion incorporation exhibits distribution of defects levels near the conduction band around ~1.5eV. These defect levels (reaction sites) determine the chemical reactivity, catalytic, electrical, optical, and mechanical properties of the Cu doped systems.

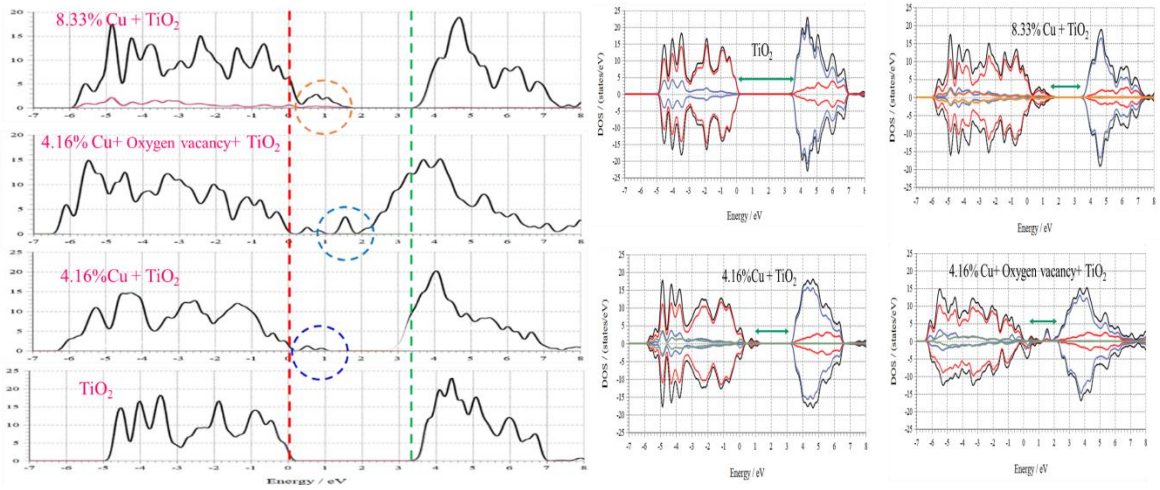

Fig.3a & 3b Density of states and partial density of states of
(a) pristine TiO_2 (b) SYS-2 (c) SYS-3 (d) SYS-4

3.2.1 Fermi Energy

The Fermi energy is the energy of the highest filled planewave state where the fermi level illustrates the occupation of energy levels at thermal equilibrium. The position of Fermi level can be affected by the produced charge compensators, carrier concentration, effective masses, temperature, and presence of Co-dopants. Thus, the presence of impurity metal ions as well

the surface defects/oxygen vacancies might change the position of fermi levels in the TiO_2 host system

since the fermilevel position can modify the charge transfer direction and the corressponding recombination kinetics in undoped and Cu doped TiO_2 material. In electronic properties investigation, the fermi energies were evaluated for all four configurations. The calculated fermi energies of pure and Cu doped TiO_2 systems are given in Table 1. The Fermi level is arbitrarily chosen as the origin of the energy [38]. The Fermi level of modeled structures were dependent on their surface defects. The fermi energy for pristine TiO_2 was 8.911 eV. However, it is seen in Cu-doped TiO_2 systems (SYS-2, SYS-3, SYS-4), the fermi energy has been reduced significantly. The Cu (4.16% and 8.33%) doped TiO_2 systems show marginally higher reduction in fermi energy compared to the fermi energy of SYS-3 (modelled with oxygen vacancy). In Cu doped TiO_2, the integrated impurity atoms act like electron acceptor since some electrons of the valence band bound to acceptor impurities leaving empty states or holes. i.e., After doping Cu atoms, (Cu has lower fermi levels than TiO_2), the TiO_2 semiconductor becomes p-type characteristic, which means the fermi energy level shifts closer to valence band to attain pseudo equilibrium [39]. In SYS-2, the fermi level has been shifted slightly about ~0.8eV above the valence band (towards conduction band), accordingly the improvement of charge mobility/charge transfer happens (offers a trapping potential well), in turn, it can limit the excitons recombination. Thus, the integrated cations (by Cu doping) act as oxidizing agents in chemical reactions. In SYS-3, the oxygen vacancies (point defects) lead to the formation of unpaired electrons (serve as deep donors). Thus, the localized electronic states are established near the conduction band minimum and acts like electron trap for the charge carriers. In addition, the energy levels from conduction band low down to touch the fermi level, which supports *n*-type behavior of the material. However, to fulfill the electrical charge neutrality, the fermi level has shifted towards the valence band. The shift observed in the fermi energy level signifies the oxygen vacancy formation greatly. Adjusting the fermi level of metal doped TiO_2 can change the charge transport path which influence the behaviors of reactants in photocatalytic oxidation process. When the Cu concentration in TiO_2 is about 8.33 at%, the Fermi level shifts above the valence band which indicates that this sample is a P-type semiconductor. It means that shallow acceptor states are created around the fermi level in the top of the valence band, leading to the increase of cation carrier concentration.

Table. 1 Fermi energy of pure and Cu doped TiO_2 systems

System	E_f (eV)
Pure TiO_2 (SYS-1)	8.9116 eV
4.16% Cu-TiO_2 (SYS-2)	7.6715 eV
4.16%Cu+oxygen vacancy+TiO_2(SYS-3)	8.4994 eV
8.33% Cu+-TiO_2 (SYS-4)	7.3088 eV

3.3 Band structure of Pure TiO_2 and Cu doped TiO_2

The electrical, optical, and magnetic properties of semiconducting materials can be delineated in terms of the band structure. It imparts the electronic levels in crystal structures, which are categorized by two quantum numbers, the Bloch vector k and the band index n. Bloch vectors provide a visual insight into the quantum states of the materials. It is an element of the reciprocal space (in units 1/length) and the energy of the electron E_n (k) is a continuous function of k, so that one obtains a continuous range of energies referred to as the energy band. The ab initio calculated electronic band structure using the density functional theory (DFT) depicted in Fig. 4 applying the localization of the excess electronic charge using +U correction. The corresponding band gap is 3.2 eV, which is in good agreement with the experiment. It is observed that the lowest point of the conduction band is located at the symmetry point G and the highest point of the valence band is located at symmetry points Y which confirm all modelled structures are indirect band gap semiconductors [40]. Therefore, the valence band electron doesn't transport directly to the conduction band and both a photon and a phonon are involved for momentum conservation.

Usually, in pristine TiO_2. the conduction band edge and the fermi level are much close to each other. In SYS-2, more bands are available near the valence band maximum. These energy bands comprised mostly the 3d states of Cu and Titanium and 2p states of Oxygen. Thus, the Cu doping leads to the development of d states near the uppermost part of the valence band and modify the energy separation between the O 2p and the Ti t2g bands of TiO_2. Oxygen vacancy (V_o) is the most important point defect in TiO_2 which make dominant contribution to the band gap states of TiO_2 surface [41]. Oxygen vacancies create fully occupied defect states near the conduction band and serve as shallow donors and plays an important role in altering the energy of levels of conduction band. Oxygen vacancy or defects created determines the

overall charge distribution of the TiO_2 material and have a dominant effect on heterogeneous catalysis. [42,43]. Removal of one oxygen from the substance leads to addition of two electrons (i.e., electron-doping) in the lattice and these electrons will be transferred to empty sates of Ti 3d states and forms Ti^{3+} centres**.** In SYS-3, it could be seen the presence of defect state about ~1eV below the conduction band which leads to the energy reduction in the mid-range of conduction band due to oxygen vacancy existence (lattice distortion). Thus, the existence of Ti^{3+} species supports the different applications like photochemical water splitting, photocatalysis, and dye sensitized solar cells [44]. In SYS-4, due to the higher concentration of Cu dopant, accumulation of larger number of holes (deficiency of electrons) moves up the Cu 3d states about ~ 0.8eV above the valence band.

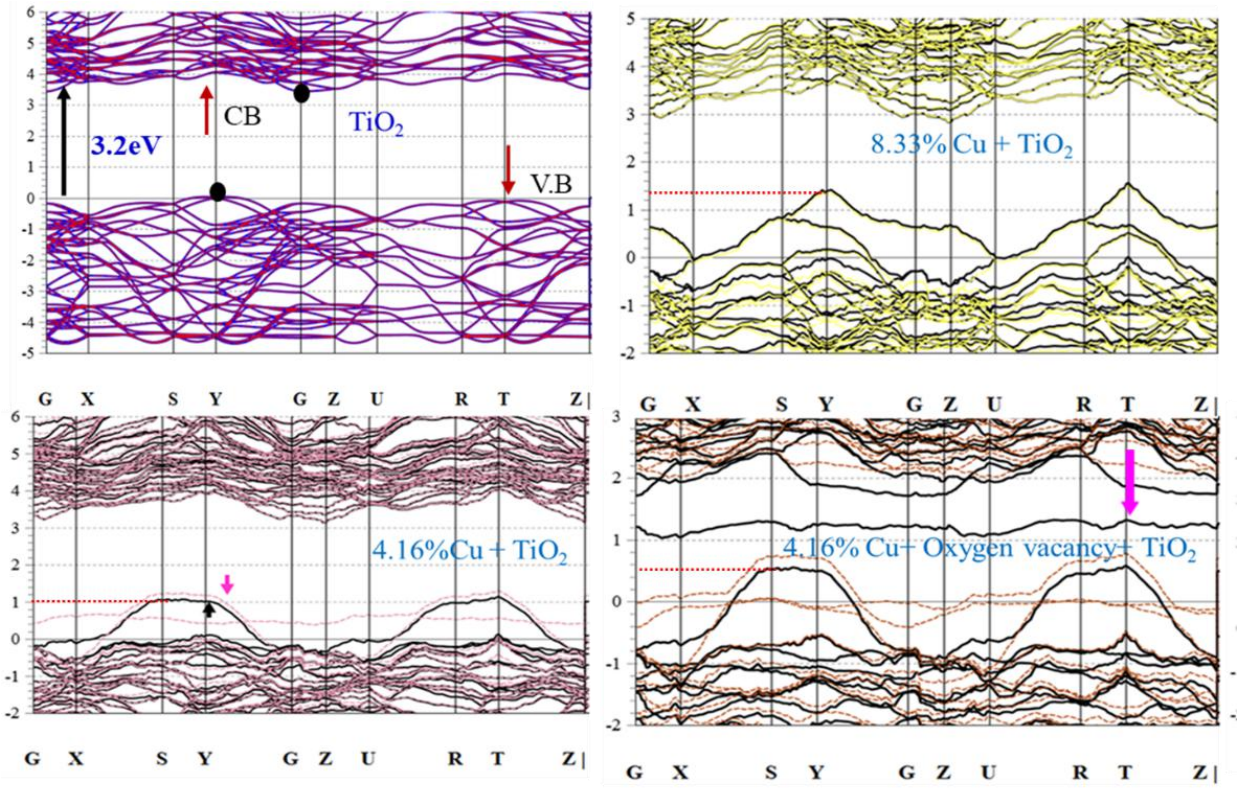

Fig.4 Band structures of (a) pristine TiO_2 (b) SYS-2 (c) SYS-3 (d) SYS-4

3.4 Magnetization

The integration of transition metal dopants like Cu, Ni, Fe and Co into the pristine TiO_2 matrix leads to an interaction between the metal ions and the delocalized electrons formed via the defects present in the TiO_2 lattice which in turn induces ferromagnetic behavior in the doped system [45]. In this work, the pristine sample do not display any magnetic nature. However, the doped SYS-2, SYS-3, SYS-4 exhibit remarkable magnetization effect. Specifically, with the higher concentration of oxygen vacancies or with the structural point

defects, Cu doped TiO_2 displays higher magnetization value. The calculated magnetization values are shown in Table 2.

Table. 2 Calculated Magnetization values of pure and Cu doped TiO_2 systems

System	Total magnetization (Bohr mag/cell)
Pristine TiO_2 (SYS-1)	0.00
4.16% Cu-TiO_2 (SYS-2)	0.67
4.16% Cu oxygen vacancy$_+$$TiO_2$ (SYS-3)	1.67
8.33% Cu-TiO_2 (SYS-4)	-0.25

4. Conclusion

All the four modelled structures were constructed from an optimized anatase phase TiO_2 unit cells.

The electronic structures and the band edge positions of anatase TiO_2 doped with Cu transition metals have been analyzed by ab initio band calculations based on the density functional theory with the planewave ultra-soft pseudopotential method. The electronic structure of transition metal oxide semiconductor TiO_2 doped with 3d transition metals Cu ions has been modified by introducing impurity energy levels at the top of valence band and band gap reduction. The hybridization of p-d molecular orbitals taken place between dopant Cu 3d states and O 2p states lead to creation of impurity levels above the valence band the overlap among the 3d states of Cu, Ti, and 2p states of oxygen, which enhances photocatalytic activity in the visible light region. Both the broadening of the valence band and Cu impurity states within the band gap might also enhance the photocatalytic activity. Here Cu doping delays electron-hole recombination and thus promotes the photo induced interfacial charge-transfer between Cu and TiO_2 energy levels. This leads to the production of more reactive species. Thus, the systems with more adsorption sites can enhance the surface contact between photo reactor dyes and doped catalyst. The produced OH and O_2^- radicals oxidize and decompose the molecules of pollutants. The enhancement in the catalytic performance of Cu doped TiO_2 metal oxide systems make them as excellent materials in the field of catalytic water splitting and purification applications.

References

[1] Fujishima A. Zhang X, Tryk DA. TiO_2 photocatalysis and related surface phenomena. Surf. Sci. Rep. 2008; 63(12):515–582.

[2] De Angelis F, Valentin CD, Fantacci S, Vittadini A, Selloni A. Theoretical Studies on Anatase and Less Common TiO2 Phases: Bulk, Surfaces, and Nanomaterials. Chem. Rev. 2014;114(19): 9708–9753.

[3] Zhan Qu, Yali Su, Li Sun, Feng Liang, and Guohe Zhang. Study of the Structure, Electronic and Optical Properties of BiOI/Rutile-TiO_2 Heterojunction by the First-Principles Calculation. Materials. **2020**;13(2):323-336

[4] Anpo M. Preparation, Characterization, and Reactivities of Highly Functional Titanium Oxide-Based Photocatalysts Able to Operate under UV–Visible Light Irradiation: Approaches in Realizing High Efficiency in the Use of Visible Light. B. Chem. Soc. Jpn., 2004; 77(8):1427-1435.

[5] Mohamed RM, Mckinney DL, Singmund WM. Enhanced nano catalysts. Mater. Sci. Eng. R-Rep., 2012; 73(1):1-13

[6] Kim TW, Ha HW, Paek MJ, Hyun SH, Choy JH, Hwang SJ. Unique phase transformation behavior and visible light photocatalytic activity of titanium oxide hybridized with copper oxide. J. Mater. Chem. 2010;20(16):3238–3245

[7] Assadi MHN, Hanaor DA. The effects of copper doping on photocatalytic activity at planes of anatase TiO_2: A theoretical study. Appl. Surf. Sci. 2016;387(5): 682–689

[8] Wu F, Hu X, Fan J, Liu E, Sun T, Kang L, Hou W, Zhu C, Liu H. Photocatalytic activity of Ag/TiO2 nanotube arrays enhanced by surface plasmon resonance and application in hydrogen evolution by water splitting. Plasmonics. 2013;8(1):501–508.

[9] Xu S, Du AJ, Liu J, Ng J, Sun DD. Highly efficient CuO incorporated TiO2 nanotube photocatalyst for hydrogen production from water. Int. J. Hydrogen Energy. 2011;36(11):6560–6568.

[10] Wu Y, Lazic P, Hautier G, Persson K, Ceder G. First principles high throughput screening of oxynitrides for water-spliting photocatalysts. Energy & Environmental Science. 2013;**6**(1):157-168.

[11] Mingyang Wu, Dan Sun, Changlong Tan, Xiaohua Tian and Yuewu Huang. Al-Doped ZnO Monolayer as a Promising Transparent Electrode Material: A First-Principles Study, Materials. 2017;10(4):359-373

[12] Mostaghni F, Abed Y. Structural determination of Co/TiO2 nanocomposite:XRD technique and simulation analysis. Materials Science-Poland. 2016; 34(3):534-539.

[13] Huamin Zhang, Xiaohui Yu, John A. McLeod, Xuhui Sun. First-principles study of Cu-doping and oxygen vacancy effects on$TiO_2$for water splitting. Chemical Physics Letters. 2014; 612(): 106–110.

[14] Koch W, Holthausen MC. A Chemist's Guide to Density Functional Theory. New York,USA: John Wiley & Sons; 2001. DOI: 10.1002/3527600043

[15] Roberto Peverati, Yan Zhao, Donald G Truhlar, Generalized Gradient Approximation That Recovers the Second-Order Density-Gradient Expansion with Optimized Across-the-Board Performance. J. Phys. Chem. Lett. 2011;2(16):1991–1997.

[16] Sarah A, Tolba, Kareem M, Gameel, Basant A, Ali, Hossam A, Almossalami, Nageh K Allam. The DFT+U: Approaches, Accuracy, and Applications.2018; Doi.org/10.5772/intechopen.72020

[17] Hohenberg P, Kohn W. Inhomogeneous Electron Gas. Phys. Rev. B, 1964;136(3B):864-0871.

[18] Kohn W and Sham L. softness, and the fukui function in the electronic theory of metals and Catalysis. J. Phys. Rev. 1965; 140(3): 1133-1138.

[19] John P Perdew, Mel Levy. Extrema of the density functional for the energy: Excited states from the ground-state theory. Phys. Rev. B. 1985; 31(10):6264

[20] Vanderbilt D. Soft self-consistent pseudopotentials in a generalized eigenvalue formalism. Phys. Rev. B. 1990; 41(11):7892-7895.

[21] Matsson AE, Schulz PA, Desjarlais MP. Designing meaningful density functional theory calculations in materials science—A primer. Modelling and Simulation in Materials Science and Engineering. 2005;13(1): 25 071003

[22] Snehamol Mathew, Priyanka Ganguly, Stephen Rhatigan, Vignesh Kumaravel, Ciara Byrne, Steven J. Hinder, John Bartlett, Michael Nolan, and Suresh C. Pillai, Cu-Doped TiO_2: Visible Light Assisted Photocatalytic Antimicrobial Activity. Appl. Sci. 2018;8(11):2067-2072.

[23] Kun Wang, Ting Peng, Zhongming Wang, Hong Wang, Xun Chen, Wenxin Dai, Xianzhi Fu, Correlation between the H_2 response and its oxidation over TiO_2 and N doped TiO_2 under UV irradiation induced by Fermi level. Applied Catalysis B: Environmental. 2019; 250(4):89–98

[24] Shun Kashiwaya, Jan Morasch, Verena Streibel, Thierry Toupance, Wolfram Jaegermann and Andreas Klein. The Work Function of TiO_2. Surfaces. 2018;1(1):73–89

[25] Kulbir Kaur Ghuman, Chandra Veer Singh. A DFT C U study of (Rh, Nb)-codoped rutile TiO_2. J. Phys. Condens. Matter. 2013;25(8):085501-085510.

[26] John R, Padmavathi S. Ab Initio Calculations on Structural, Electronic and Optical Properties of ZnO in Wurtzite Phase. Crystal Structure Theory and Applications. 2016;**5(2):** 24-41.

[27] Yaqin Wang, Ruirui Zhang, Jianbao Li, Liangliang Li and Shiwei Lin, First-principles study on transition metal-doped anatase TiO_2. Nanoscale Research Letters. 2014;9(8):46-52.

[28] Dorian AH, Hanaor, Mohammed HN. Assadi, Sean Li, Aibing Yu, Charles C. Sorrell. Ab Initio Study of Phase Stability in Doped TiO_2. Computational Mechanics. 2012; 50 (2):185-194.

[29] Wang Y, Perdew JP. Spin scaling of the electron-gas correlation energy in the high-density limit. Phys. Rev. B. 1991; 43(11): 8911-8916.

[30] Baroni S, Dal Corso A, de Gironcoli S, Giannozzi P, Cavazzoni C, Ballabio G, Scandolo S, Chiarotti G, Focher P, Pasquarello A, Laasonen K, Trave A, Car R, Marzari N, Kokalj A. Journal of Physics: Condensed Matter. 2009;21()39. **http://www.pwscf.org**

[31] Perdew JP, Ruzsinszky A, Csonka GI, Vydrov OA, Scuseria GE, Constantin LA, Zhou X, Burke K. Restoring the density-gradient expansion for exchange in solids and surfaces. Phys.Rev. Lett. 2008;100(13):136406.

[32] Perdew JP, Burke K, Ernzerhof M. Generalized Gradient Approximation Made Simple. Phys. Rev. Lett. 1996;77(18):3865−3868.

[33] Arroyo-de Dompablo ME, Morales-García A, Taravillo M. DFT+U calculations of crystal lattice, electronic structure, and phase stability under pressure of TiO_2 polymorphs. Journal of chemical physics 2011;135(5):054503

[34] Ma X., Lu B, Li D, Shi R, Pan C, Zhu Y. Origin of photocatalytic activation of silver orthophosphate from first-principles. J. Phys. Chem. C 2011;115(11):4680–4687.

[35] Navas J, Sánchez-Coronilla A, Aguilar T, Hernández NC, Desireé M, Sánchez-Márquez J, Zorrilla D, Fernández-Lorenzo C, Alcántara R, Martín-Calleja J. Experimental and theoretical study of the electronic properties of Cu-doped anatase TiO_2 . Phys. Chem. Chem. Phys. 2014;16(8): 3835–3845.

[36] Nurul Fajariah, Wahyu Aji Eko Prabowo, Fadjar Fathurrahman, Asih Melati, Hermawan Kresno Dipojono. The investigation of electronic structure of transition metal doped TiO_2 for diluted magnetic semiconductor applications: A first principles study. Procedia Engineering. 2017; 170 (1):141 – 147

[37] Ivan Mora-Sero, Juan Bisquert. Fermi Level of Surface States in TiO_2 Nanoparticles, Nano Lett., 2003;3(7): 945–949.

[38] Charlene Chen, Kai-Chen Cheng, Evgeniy Chagarov, and Jerzy Kanicki. Crystalline In–Ga–Zn–O Density of States and Energy Band Structure Calculation Using Density Function Theory. Japanese Journal of Applied Physics. 2011;50 (9): 091102.

[39] Li L, Meng F, Hu X, Qiao L, Sun CQ, Tian H, et al. TiO_2Band Restructuring by B and P Dopants. PLoS ONE. (2016);11(4): e0152726

[40] Hongfei Li, Yuzheng Guo, John Robertson. Calculation of TiO_2 Surface and Subsurface Oxygen Vacancy by the Screened Exchange Functional. The Journal of Physical Chemistry C. 2015; 119 (32):18160-18166

[41] Jia J, Qian C, Dong Y, Li YF, Wang H, Ghoussoub M, Butler KT, Walsh A, Ozin GA. Heterogeneous catalytic hydrogenation of CO_2 by metal oxides: defect engineering perfecting imperfection. Chem. Soc. Rev. 2017;46(1): 4631−4644.

[42] Widmann D, Behm RJ, Activation of molecular oxygen and the nature of the active oxygen species for co oxidation on oxide supported au catalysts. Acc. Chem. Res. 2014;47(3):740−749

[43] Puigdollers AR, Schlexer P, Tosoni S, Pacchioni G. Increasing oxide reducibility: The role of metal/oxide interfaces in the formation of oxygen vacancies. ACS Catal. 2017;7(10):6493−6513.

[44] Yoyo Hinuma, Takashi Toyao, Takashi Kamachi, Zen Maeno, Satoru Takakusagi, Shinya Furukawa, Ichigaku Takigawa, and Ken-ichi Shimizu. Density Functional Theory Calculations of Oxygen Vacancy Formation and Subsequent Molecular Adsorption on Oxide Surfaces. J. Phys. Chem. C 2018;122(51): 29435−29444

[45] Hsin-Yi Lee, Stewart J Clark, John Robertson. Calculation of point defects in rutile TiO_2 by the Screened Exchange Hybrid Functional. Phys. Rev. B. 2012;86(7): 075209